

${}^2E \rightarrow {}^2T_2$ Absorption Spectrum of Ruby*G. K. KLAUMINZER,[†] P. L. SCOTT,[‡] AND H. W. MOOS[§]
Department of Physics, Stanford University, Stanford, California

(Received 3 September 1965)

Four of the six possible components in the sharp-line absorption spectrum ${}^2E(t_2^3) \rightarrow {}^2T_2(t_2^3)$ have been observed in a sample of 0.05% ruby cooled to 95°K. The measured wavelengths and linewidths of the transitions are identical, within experimental error, to those calculated on the basis of observed absorptions to each of the excited levels from the 4A_2 ground state. The polarizations and relative strengths of the transitions are in good agreement with the existing crystal-field-theory predictions of Tanabe and Sugano.

I. INTRODUCTION

BECAUSE so many of the predicted levels have been observed, the optical spectrum of ruby ($\text{Al}_2\text{O}_3:\text{Cr}^{3+}$) is a particularly interesting example of a transition-metal ion in a crystal. Recently, Gires and Mayer,¹ by populating the metastable 2E states in a manner similar to that described in this paper, observed absorption bands from the 2E states in the visible and ultraviolet. They suggested that these bands might be transitions to doublet levels predicted by the crystal-field theory of Sugano and Tanabe.² These levels would normally not be observed from the 4A_2 ground state owing to the change in spin. Naiman and Linz³ in optical-absorption measurements from the ground state in concentrated (0.35%) ruby at 4.2°K show weak absorption bands which they attribute to doublet bands predicted by the crystal-field theory. Their data is in agreement with that of Gires and Mayer although their crystal has a rather large Cr^{3+} concentration and their absorption spectrum contains considerable structure.

The purpose of this paper is to report a study of the absorption between the metastable ${}^2E(t_2^3)$ and the ${}^2T_2(t_2^3)$ states.^{3a} Although the transitions take place in the infrared at $1.5\ \mu$ and are slightly more difficult to study they are interesting because they are fine lines. Furthermore, they are the only observed fine-line transitions in ruby which are spin-allowed. (In fact, to the best of our knowledge these are the only observed fine-line transitions in a transition-metal ion which are

spin-allowed.⁴) Thus the values of the oscillator strength are of some interest. Our experimental technique, the data, and its correlation with existing theory are described in the following paragraphs.

II. EXPERIMENTAL DETAILS

A diagram of the apparatus is shown in Fig. 1. The sample is a Linde 0.05% ruby cylinder, $\frac{1}{2}$ in. in diameter and 2 cm in length with the optic axis perpendicular to the cylinder axis. The ends are polished while the sides are left rough to aid in producing uniform pumping. The sample is placed in a small Dewar, which in

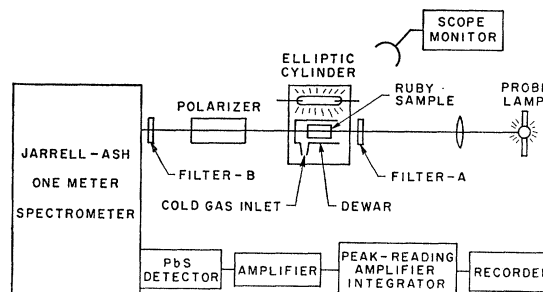


FIG. 1. A diagram of the apparatus.

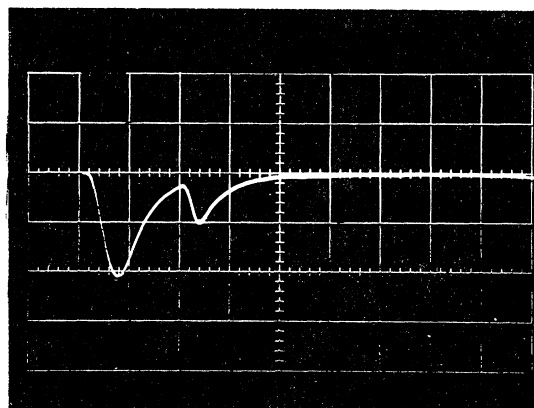


FIG. 2. The scope monitor output, showing the probe pulse following the pump pulse. The relative sizes of the two pulses have no significance.

* Work supported by the U. S. Office of Naval Research Contract Nonr 225(78).

[†] 1st Lt., United States Air Force presently at McClellan Air Force Base, California; National Science Foundation Pre-doctoral Fellow.

[‡] Alfred P. Sloan Foundation Fellow.

[§] Present address: Department of Physics, Johns Hopkins University, Baltimore, Maryland.

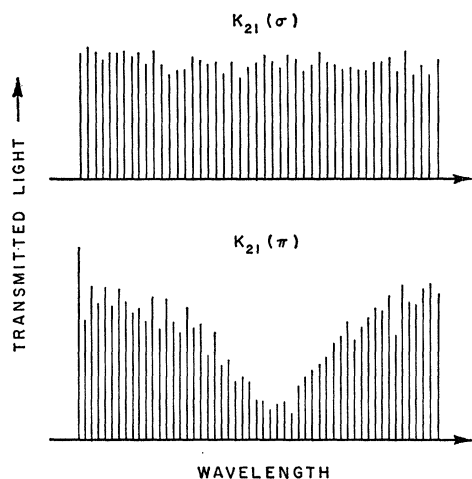
¹ F. Gires and G. Mayer, *Compt. Rend.* **254**, 659 (1962); *Ann. Radioelectricité* **18**, 112 (1963).

² S. Sugano and Y. Tanabe, *J. Phys. Soc. Japan* **13**, 880 (1958); Y. Tanabe and S. Sugano, **9**, 753 (1954).

³ C. S. Naiman and A. Linz, in *Proceedings of the Symposium on Optical Masers*, (Polytechnic Press, Brooklyn, New York, 1963) p. 369.

^{3a} Note added in proof. Similar results on the infrared absorption spectrum of 1.6% ruby at room temperature have been reported recently. [T. Kushida, *J. Phys. Soc. Japan* **20**, 619 (1965).] Their results are in substantial agreement with those reported here.

⁴ See, for instance, Table I of S. Sugano, *Progr. Theoret. Phys. (Kyoto)*, Suppl. **14**, 66 (1960).

FIG. 3. Raw data showing absorption in the K_{12} line.

turn is placed in an elliptic cylinder with a PEK Xe 14-C-3 xenon flash lamp. The lamp is powered by a 240- μ F capacitor bank, typically charged to 1000 volts prior to flashing. The sample may be cooled to 85°K by blowing cold nitrogen gas past it. The probe lamp is a PEK 500-W xenon short arc operated continuously at 300 W and pulsed 2 msec after the pumping flash to provide a peak output of approximately 25 kW. Figure 2 shows a typical output of the scope monitor (which merely detects the scattered visible light) showing the probe pulse following the pump pulse.

The spectrometer is a Jarrell-Ash 1M Ebert scanning monochromator, used in fourth order. The resolving power is such that negligible broadening is contributed by the spectrometer. The detector is a Kodak type *N* PbS infrared detector with a response time of 0.3 msec.

The experimental technique is as follows: With the spectrometer scanning slowly, the pumping flash lamp is fired every 10 sec. Two msec after each firing, the probe lamp is fired through a delayed trigger network. All wavelengths shorter than one μ are immediately filtered from this pulse (filter A, Fig. 1) to avoid additional pumping of the sample. After traversing the sample, the probe light is polarized with a Glan-Thompson prism, and then sent into the spectrometer through appropriate filters B which eliminate unwanted orders. The signal from the detector is amplified 1000 times and then sent to an integrating circuit which

TABLE I. Wavelengths and linewidths of the K lines.

Line	Wavelength		Linewidth	
	Observed (\AA)	Calculated (\AA)	Observed (cm^{-1})	Calculated (cm^{-1})
K_{11}	$15\,204.7 \pm 0.3$	15 204.74	5.9	5.7
K_{12}	$15\,036.2 \pm 0.3$	15 036.42	7.1	7.2
K_{21}	$15\,274.0 \pm 0.3$	15 273.9	5.8	5.7
K_{22}	$15\,104.0 \pm 0.3$	15 104.1	6.7	7.2

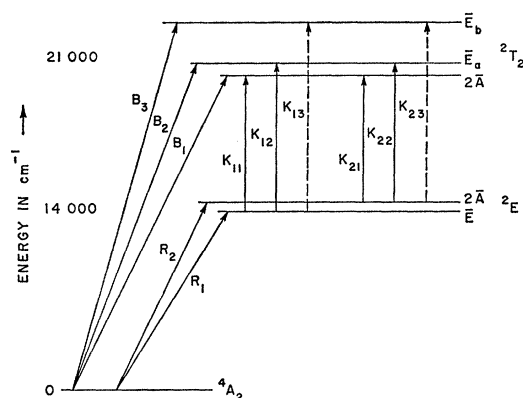


FIG. 4. The ruby energy levels relevant to this experiment. The diagram is not to scale.

stores the pulse on a condenser and integrates the condenser voltage. This lengthened pulse is then easily followed by a pen recorder. Linearity of the entire system is checked with neutral density filters. A sample of the resulting traces is shown in Fig. 3; each spike represents one pulse from the probe lamp.

III. RESULTS AND DISCUSSION

An energy-level diagram with the relevant energy levels is shown in Fig. 4. In addition to the R and B lines first named by duBois and Elias,⁵ are shown the newly observed lines, which we have termed the K lines. Figure 5 shows the profiles for each of the observed lines as deduced from data similar to that of Fig. 3. Each of the lines appeared in one polarization only. In Table I are listed the observed wavelengths and linewidths of the K lines, as well as wavelengths and linewidths calculated from the previously observed R and B lines ($T=95^\circ\text{K}$). The observed and expected

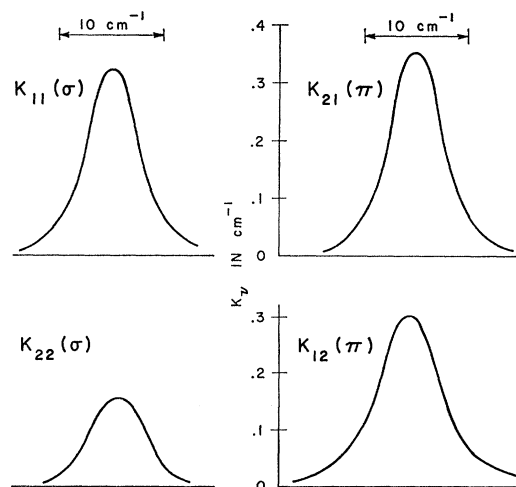


FIG. 5. Absorption profiles for the four observed lines.

⁵ H. duBois and G. J. Elias, *Ann. Physik* **27**, 233 (1908).

values agree within experimental error. We observed no absorption corresponding to the K_{13} or K_{23} lines; it is probable that these transitions are considerably weaker than the others.

The polarizations, and to some extent the relative

intensities of the transitions may be calculated using the methods of Sugano, Tanabe, and Kamimura^{2,6} for both electric and magnetic dipole transitions.

The electric dipole matrix element for the K_{12} transition, for example, is given by

$$\begin{aligned} & \langle {}^2T_{2g}x - |P_z(T_{1u}a_0)| {}^2E_gu - \rangle \\ &= \sum_{\Gamma u, \gamma} \langle {}^2T_{2g}x - |V_0(T_{1u}a_0)| {}^2\Gamma_u \gamma \rangle \langle {}^2\Gamma_u \gamma |P_z(T_{1u}a_0)| {}^2E_gu - \rangle / [W({}^2E_g) - W({}^2\Gamma_u)] \\ &+ \sum_{\Gamma u, \gamma} \langle {}^2T_{2g}x - |P_z(T_{1u}a_0)| {}^2\Gamma_u \gamma \rangle \langle {}^2\Gamma_u \gamma |V_0(T_{1u}a_0)| {}^2E_gu - \rangle / [W({}^2T_{2g}) - W({}^2\Gamma_u)], \quad (1) \end{aligned}$$

where $V_0(T_{1u}a_0) = k \sum z_i$ is the static hemihedral crystal field at a Cr^{3+} site. The notation is that of Sugano and Tanabe.³ Equation (1) may be simplified by making use of Clebsch-Gordan coefficients tabulated by Tanabe and Kamimura,⁶ thus allowing us to predict selection rules and, to some extent, the relative intensities of the transitions. The results are displayed in Table II, along with the experimentally observed polarizations and intensities.

We conclude that the transitions are electric dipole, as magnetic dipole transitions would have polarizations opposite to those observed. Because of our lack of knowledge of the nature of the intermediate odd states in Eq. (1), we can only say, on the basis of the simple theory, that the intensity ratios π/σ and π/σ' should lie between $\frac{1}{2}$ and infinity. The agreement between theory and experiment may perhaps be improved through a more exact determination of the state vectors, including configuration interactions, as suggested by the calculations of Macfarlane⁷ and Sugano and Peter.⁸ Such a determination was not done here, however.

The observed oscillator strength f (summed over the group of transitions ${}^2E \rightarrow {}^2T_2$) may be roughly calcu-

lated using the formula⁹

$$f = \frac{nmc}{\pi e^2 N} \left(\frac{E_0}{E_{\text{eff}}} \right)^2 \int k_\nu dv, \quad (2)$$

where n is the index of refraction of the medium, m and e are the mass and charge of the electron, c is the velocity of light, N is the number of excited chromium ions per cm^3 , E_0 is the average radiation field in the medium, E_{eff} is the radiation field at the site of a chromium ion, and k_ν is the absorption coefficient, i.e., $I(\nu) = I_0(\nu)e^{-k_\nu x}$. The local field correction is approximately given by the Lorentz local field ratio $E_0/E_{\text{eff}} = 3/(n^2 + 2)$. By observing the change in transmitted light at the center of the green absorption band (${}^4A_2 \rightarrow {}^4T_2$) as the sample was pumped, we found that about 3.5% of the chromium ions were excited at our 120-joule pumping level. Substitution of observed absorption coefficients and linewidths into Eq. (2) yields the approximate result $f = 1 \times 10^{-5}$. The excited-state population estimate was made on the assumption that no absorption from the 2E state was present. Thus we may have underestimated the excited-state population, and overestimated the oscillator strength. We have not made a theoretical estimate for f , again primarily because of our lack of knowledge concerning the nature of the intermediate odd states in Eq. (1), which serve to break the parity selection rule. On the other hand, we expect a larger value here than for the R lines or the B lines, since the K lines are spin-allowed, whereas the R and B lines are spin-forbidden.

IV. CONCLUSION

The observed ${}^2E(t_2^3) \rightarrow {}^2T_2(t_2^3)$ optical absorption in ruby seems reasonably well explained by existing theory based on the crystal-field model. The measured oscillator strength, $f \cong 1 \times 10^{-5}$ is of interest. Although, as is expected, it is stronger than the usual spin-forbidden fine lines, it is an order of magnitude less than the values of the spin-allowed broad bands.

⁹ D. L. Dexter, *Solid State Phys.* **6**, 353 (1958).

TABLE II. Polarizations and intensities of the K lines.

Line	Observed ^a σ	$k_{\nu\text{max}}$ in cm^{-1} π	Predicted polarization and intensity
K_{11}	0.26	0	σ
K_{12}	0	0.24	π
K_{13}	<0.1	<0.1	σ'
K_{21}	0	0.43	π
K_{22}	0.19	0	σ
K_{23}	<0.1	<0.1	σ'

^a These values have been corrected to account for the Boltzmann distribution in the 2E state.

⁶ Y. Tanabe and H. Kamimura, *J. Phys. Soc. Japan* **13**, 394 (1958).

⁷ R. M. Macfarlane, *J. Chem. Phys.* **39**, 3118 (1963).

⁸ S. Sugano and M. Peter, *Phys. Rev.* **122**, 381 (1961).

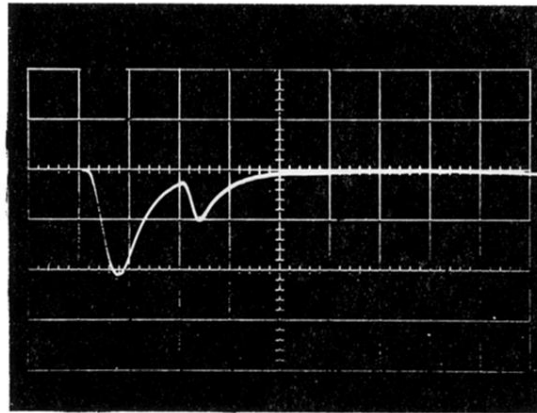


FIG. 2. The scope monitor output, showing the probe pulse following the pump pulse. The relative sizes of the two pulses have no significance.